Nonequilibrium Particle Morphology Development in Seeded Emulsion Polymerization. II. Influence of Seed Polymer T_g

Lina E. Karlsson,[1] Ola J. Karlsson,[1] Donald C. Sundberg[2]

[1]*Department of Polymer Science & Engineering, Lund University, P. O. Box 124, 22100 Lund, Sweden*
[2]*Polymer Research Group, Department of Chemical Engineering, University of New Hampshire, Durham, New Hampshire 03824*

Received 20 May 2002; accepted 15 January 2003

ABSTRACT: Most structured latex particles are formed in the nonequilibrium state as a result of the reaction kinetics proceeding faster than the phase separation kinetics. Of the many factors controlling such morphologies, the polarity and glass transition temperature (T_g) of the seed polymer are important. In order to study the direct effect of the seed polymer T_g on morphology, we produced a series of poly(methyl methacrylate)/poly(methyl acrylate) seed copolymers having glass points between 52 and 98°C, and particle sizes between 320 and 390 nm. We then used styrene as a second-stage monomer reacting in both the batch and semibatch process modes, and utilized reaction temperatures (T_r) between 50 and 70°C. Monomer feed rates were varied between flooded and starve-fed conditions. The equilibrium morphology for these composite particles is an inverted core–shell structure, but all morphologies obtained in our experiments were nonequilibrium. Under monomer starved conditions only core–shell structures were formed when $(T_r - T_g) < 0$, but significant penetration of the polystyrene into the acrylic core occurs when $(T_r - T_g) > 15$°C. These results are reasonably well predicted using the "fractional penetration" model developed earlier. © 2003 Wiley Periodicals, Inc. J Appl Polym Sci 90: 905–915, 2003

Key words: latex; morphology; nonequilibrium; diffusion; core–shell; glass transition temperature

INTRODUCTION

The control of latex particle morphology has always been of prime importance in industry as many properties of the final products depend upon the composite structure of the latex particles. Coatings and impact modifiers are good examples of such products. Increasingly there have been literature reports of both experimental studies and modeling efforts related to morphology development in a variety of different emulsion polymer systems. While most of the experimental results likely produced nonequilibrium structures, most of the modeling efforts have been related to equilibrium conditions. The nonequilibrium modeling work of Gonzalez-Ortiz and Asua[1–3] and Stubbs et al.[4] are notable exceptions. In the present work nonequilibrium conditions are again considered.

It has become clear[4,5] that the mobility of the entering oligomeric radical within the particle has a great deal to do with the ultimate morphology. This mobility is dependent on the reaction temperature and seed polymer glass transition temperature (T_g), as well as the monomer concentration within the particle. If the diffusion of the polymeric radicals within the particles is sufficiently faster than the reaction rate, the morphology is determined by the balance of interfacial forces.[6,7] Conversely, nonequilibrium conditions occur when diffusion is slow compared to reaction rates. Such conditions are often referred to as kinetically controlled. The goal of this study was to determine the influence of the seed polymer T_g on the mobility of the entering oligomeric radical and its ability to penetrate towards the core of the latex particle, thereby influencing the morphology. Experiments were designed to systematically investigate the interaction between the seed polymer T_g, the reaction temperature (T_r), and the monomer concentration within the particle as they collectively determine the polymer radical mobility. The basic conditions chosen were those of a polar seed polymer and a nonpolar second stage monomer reacting in both batch and semibatch process modes. The equilibrium morphology for such systems can be designed to be an inverted core–shell and thus nonequilibrium structures can become readily apparent.

Correspondence to: D. C. Sundberg (dcs@christa.unh.edu).
Contract grant sponsor: University of New Hampshire Latex Morphology Industrial Consortium (AtoFina, Neo-Resins, BASF, DSM Research, ICI Paints, Mitsubishi Chemical, and Wacker-Chemie).
Contract grant sponsor: Swedish Foundation for International Cooperation in Research and Higher Education (STINT).

EXPERIMENTAL

Materials

Methyl methacrylate (MMA, Aldrich), methyl acrylate (MA, Arcos), and styrene (St, Aldrich) were purified from inhibitors by passing them through a column packed with aluminum oxide active base (Fisher). The cleaned monomers were stored at −10°C before use. Boiled, deionized water was used in the reactions. Potassium persulfate (KPS, Fisher) and sodium bicarbonate ($NaHCO_3$) were used as initiator and buffer, respectively.

Preparation of seed lattices

Seed latices were prepared by surfactant-free, batch emulsion copolymerization at 80°C in a one liter glass reactor. Recipes are given in Table I. The reactor was kept under a nitrogen blanket throughout the reactions. The solids contents of the latices were between 7 and 10% (wt). The mass of initiator used was 0.8 g KPS/100 g monomer for the 10% solids latices and 1.1 g KPS/l00 g monomer for those at 7% solids.

The water and buffer were added to the reactor after it had been purged with nitrogen for 30 min. During heating, the monomer was added, with the addition of the KPS when the temperature was stable at 80°C. As indicated in Table I, four seed latices were made at different ratios of MMA to MA to obtain seed polymer T_gs varying from about 50 to 100°C.

Second-stage polymerizations

The second-stage polymerizations were carried out in a 250 mL reactor with a continuous feed of St monomer. Reactor mixing was accomplished with a magnetic stirring bar operating at an rpm high enough to prevent any monomer pooling. The reaction temperature was 50, 60, or 70°C, depending upon the purpose of the experiment. The KPS was added at the beginning of the reaction and its amount designed to create a radical flux to the particles of $4 \cdot 10^{13}$ radicals/(m^2 s), where the area refers to the total seed particle surface area. This resulted in a flux of about 10 radicals/s to each particle. The stage ratio (wt/wt) between the seed polymer and the second-stage monomer was 1:1 in all reactions. A motor-driven syringe pump was used to feed the St monomer over different periods of time.

In order to have total control over the initiator concentration in the second-stage reactions, the residual initiator from the seed latices had to be dealt with. This residual level was calculated based on the following equation:

$$I = I_0 * exp(-k_d * t) \quad (1)$$

where I_0 and I are the initiator concentrations at the start and after time t, respectively, and k_d is the dissociation rate coefficient {taken as $k_d = (8.0 * 10^{15}) \exp[(-135{,}000\ \mathrm{J/mol})/RT]$, s^{-1}, after ref. 8}. The residual KPS in the seed latices was reduced to $I/I_0 = 0.01$ by heating the latex at 80°C for appropriate periods of time, as calculated by eq. (1).

Analysis of the latices

Quasi-elastic light scattering (QELS)

During the seed and second stage polymerizations latex samples were withdrawn for solids content determination and calculation of monomer conversion. Particle sizes were determined by QELS with a Coulter Nano-sizer.

Differential scanning calorimetry (DSC)

The T_gs of the seed polymers were determined via DSC of latex samples dried at room temperature. The instrument used was a Perkin Elmer DSC-4 and the samples were analyzed between 20 and 150°C with a heating rate of 10°C/min. In all cases the second heating cycle was used for the analysis.

Nuclear magnetic resonance (NMR)

The molar ratios of poly(methyl methacrylate) (PMMA): poly(methyl acrylate) (PMA) in the seed latices were determined with proton NMR (Bruker AM 360 MHz at ambient temperature). The dried latex polymer was dissolved at 1 wt % in deuterated chloroform. The compositional data from the NMR were also used to

TABLE I
Recipes for Seed Polymerization

Seed number	MMA/MA ratio (wt/wt)	MMA (g)	MA (g)	Water (g)	KPS[a] (mol/L) · 10^3	$NaHCO_3$[a] (mol/L) · 10^3
LEI-18	80/20	56.1	14.1	930	3.2	6.5
LEI-10	70/30	49.0	21.1	930	3.2	6.4
LEI-4	60/40	60.0	40.1	900	3.3	6.7
LEI-36	40/60	28.8	42.0	930	3.2	6.4

[a] Based on water.

TABLE II
Seed Latex Characteristics

Seed latex	Particle Diameter (nm)	Solids (wt %)	T_g (via DSC) (°C)	NMR Wt/Wt PMMA/PMA	T_g (calc) Fox (°C)
LEI-18	330	7.2	98	81/19	93
LEI-10	320	6.0	88	77/23	88
LEI-4	390	9.8	77	68/32	78
LEI-36	380	7.1	—	43/57	52

calculate the T_g via the Fox equation[9] to compare with the DSC results.

Transmission electron microscope (TEM)

The morphologies of the composite latex particles were examined with an Hitachi H600 TEM. Both whole particles and microtomed sections were examined. The latter were prepared from dried polymer samples embedded in epoxy (EPON 812) and sectioned with a diamond knife in an LKB ultramicrotome. For staining the PSt, ruthenium tetroxide vapor was used, prepared from ruthenium(III) chloride hydrate dissolved in sodium hypochlorite (Chlorox) solution. In the TEM micrographs the second-stage PSt phase appears dark and the PMMA/PMA seed polymer appears as the bright phase.

Table II lists the particle size, solids content, T_g, and compositional data obtained for the four seed latices.

RESULTS AND DISCUSSION

For the PMMA/PMA seed latices used in these experiments, the addition of St as a second-stage monomer creates a situation such that with no added surfactant (colloidal stability via the sulfate end groups), the balance of interfacial tensions (γ_{ij}) at full conversion and at equilibrium should create an inverted core–shell particle. Using eq. (2) to compute the Gibbs free energy of all possible equilibrium morphologies.

$$\Delta G = \Sigma(\gamma_i)\ (A_i) \qquad (2)$$

with $\gamma_{P1/w}$ = 17.1, $\gamma_{P2/w}$ = 32.0, and $\gamma_{P1/P2}$ = 2.16 mN/rm, the equilibrium-inverted core–shell prediction is confirmed. The polymer/water interfacial tension values were estimated by the techniques described by Dong,[10] and the polymer/polymer interfacial tension was estimated via the harmonic mean equation.[11] These values apply to a seed polymer at a PMMA:PMA ratio of 80:20. Figure 1 shows a free energy surface for all possible equilibrium morphologies[12] for this composite polymer system, with the free energy of a core–shell arrangement located at the upper left-hand corner of the surface, and that of an inverted core–shell arrangement at the lower right-hand corner. All other possible morphologies are somewhere else on the surface. This confirms that this system strongly favors an inverted core–shell morphology at thermodynamic equilibrium. In turn, this creates a convenient situation with which to study nonequilibrium morphologies, as the second-stage polymer may position itself anywhere between the periphery of the composite particle and its core, depending on how far it penetrates the seed particle. This is depicted in Figure 2, where the black phase is the polystyrene (PSt) and the white phase is the acrylic

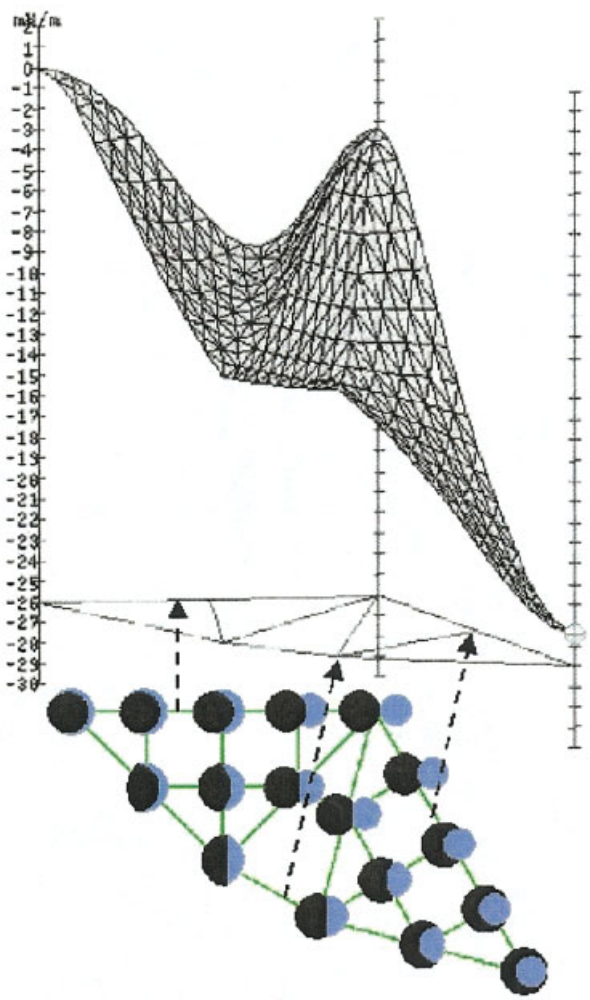

Figure 1 Gibbs free energy surface for all possible equilibrium particle morphologies based upon a 80/20 PMMA/PMA seed copolymer and a PSt second stage at a stage ratio (wt/wt) of 1:1.

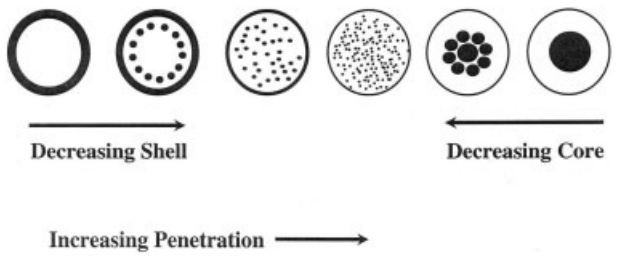

Figure 2 Schematically drawn particle morphologies and second-stage polymer penetration as expected from a polar seed and a nonpolar second-stage polymer. The light phase represents the seed polymer and the dark phase represents the second-stage polymer (ref. 4, reproduced with permission).

seed polymer. High PSt radical mobility will thus favor the morphologies depicted on the right side of the diagram and low mobilities, those on the left.

Figure 3 depicts the diffusion coefficient for a monomer unit in a polymer solution at any $(T_r - T_g) = \Delta T$ and at any polymer weight fraction, W_p.[13] Here it is very clear that the combination of monomer concentration, T_r and T_g (of the seed polymer) will create extraordinarily different conditions of mobility for the monomer, especially at weight fractions of polymer above 0.75. This is quite a common situation in second-stage reactions with slow monomer feed rates. Since we are concerned with the mobility of the entering (and then propagating) oligomeric radical, the appropriate diffusion coefficient can be several to many orders of magnitude lower than that of the monomer. We account for this by taking the polymer center of mass diffusion coefficient (as a function of chain length, i), $D_{i,\mathrm{com}}$, to be related to chain length and the monomer diffusion coefficient, D_m, as[14]

$$D_{i.com} = D_m / i^2 \tag{3}$$

This describes the center of mass mobility of the polymer radical chain in the seed polymer at the appropriate conditions. Clearly, the effect of chain length on the diffusivity of the growing radical chain can be very significant. Chains of 1000 repeat units will diffuse a million times more slowly than a monomer unit. Under very restricted diffusion, the appropriate diffusion coefficient is that given by "reaction diffusion," D_{rd}, and both should be applied simultaneously as $D_i = D_{i,\mathrm{com}} + D_{rd}$. The computational description of such penetration possibilities has been reported by Stubbs.[4]

Batch reactions

To illustrate how dramatically the mobility of the polymer radical that enters the particle from the aqueous phase can influence the final morphology of the composite latex particle, it is interesting to compare the structures obtained for batch reactions operated in two different modes. The first mode was the rather traditional batch reaction where all of the monomer was added to the seed latex and allowed to swell the particles for several hours to assure uniform monomer concentration within the particle at the chosen stage ratio (here 1:1), for a W_p of 0.5. The second mode was the same except that the second-stage initiator was added just as soon the monomer addition was complete, thus not waiting for any intentional period for monomer swelling. All of these reactions were conducted at 70°C.

Figures 4, 5, and 6 show the TEM micrographs of the stained and sectioned composite particles related to acrylic seed polymers having T_gs of 98, 88, and 77°C (via DSC), respectively. In each figure the "a" micrograph represents the swelled batch initial condition while the "b" micrograph represents the unswelled batch initial condition. In all cases, the morphologies have not reached complete equilibrium as evidenced by the numerous, large PSt domains within the light acrylic phase. In Figure 4 for the seed polymer T_g of 98°C we can see that there is a dramatic difference between the morphologies resulting from the two different versions of the batch reaction. Here the unswelled batch process, even with all of the monomer available within the reactor at the beginning, resulted in a nearly core–shell structure, while the swelled condition produced large PSt domains throughout the particles. In reference to Figure 2 we can see that the penetration of the PSt radicals must have been more restricted when the monomer was not allowed enough time to swell the particles with all of the monomer. This result is similar to that reported by Stubbs et al.[4] for the same contrasting experiments but using pure PMMA as the seed polymer (T_g = 119°C). In contrast,

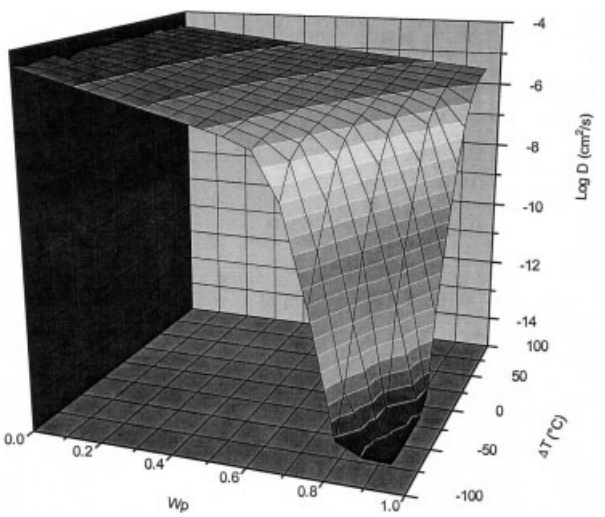

Figure 3 Diffusion coefficient of monomers in polymers as a function of weight fraction polymer (W_p) and ΔT $(T - T_g)$ (ref. 13, reproduced with permission).

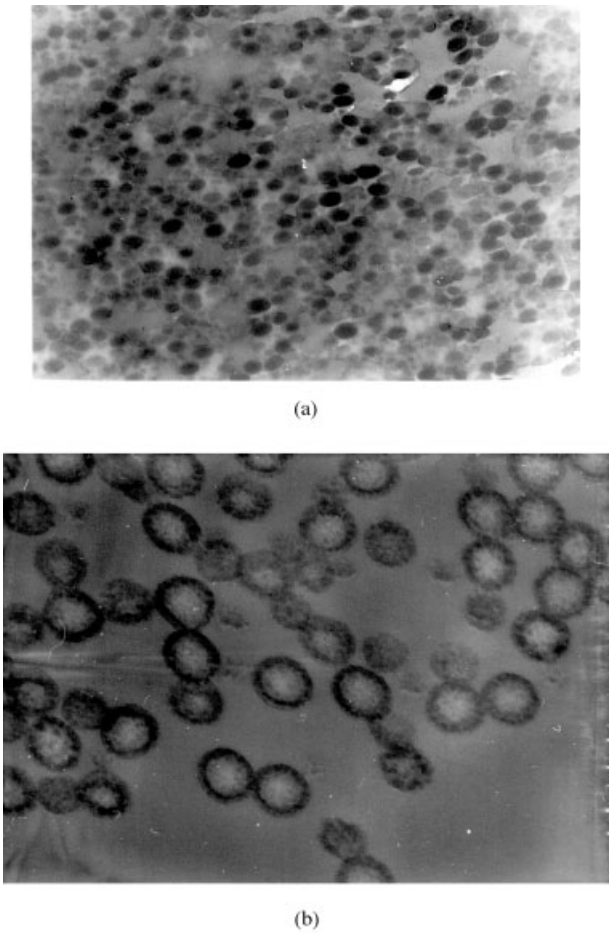

Figure 4 TEM photos of sectioned and stained samples of composite particles for the 80/20 PMMA/PMA seed polymer at T_g = 98°C. (a) Batch reaction with preswelled monomer; (b) batch reaction with unswelled monomer. Magnification 40,000×.

when the seed polymer T_gs were 88 and 77°C, there were no differences in the morphologies produced by the different versions of the batch reactions. Given these results and that the unswelled batch reaction process represents the high feed rate limit of the monomer feed, or semibatch process, we should expect to see some variations in morphology for the semibatch process studies using the various seed copolymers.

Semibatch reactions

In all of the semibatch reactions the monomer feed rates were determined so as to have the same amount of monomer fed per hour to each seed latex, based upon the particular solids content of the seed latex. In addition, all reaction recipes were based on a total second -stage monomer to seed polymer ratio (wt/wt) of 1.0. This guaranteed that from reaction to reaction, the same feed conditions applied so that direct comparisons between different seed latex experiments were possible. Accordingly we used three different feed rates in our experiments—the volume of monomer fed per hour was 0.13, 0.3 or 1.0 times the volume of the seed polymer in the reactor. The actual length of time over which the monomer was fed in each case to each seed latex was fairly close, and so for purposes of further discussion we will use monomer feed times of 9.6, 4.2, and 1.25 h to correspond to the 0.13, 0.3, and 1.0 feed conditions noted above.

We find it useful to discuss the morphology results in several different ways, beginning with the differences obtained as the monomer feed rates and seed polymer T_gs were varied. Using the batch reaction TEM photos in Figures 4–6 to represent the fastest feed rate (i.e., a zero hour feed time) as a basis, Figure 7(a–g) displays the TEM results for the four different seed latices as the monomer feed rates vary further. Given the differences for the two batch reaction conditions shown in Figure 4 for the 98°C T_g seed polymer

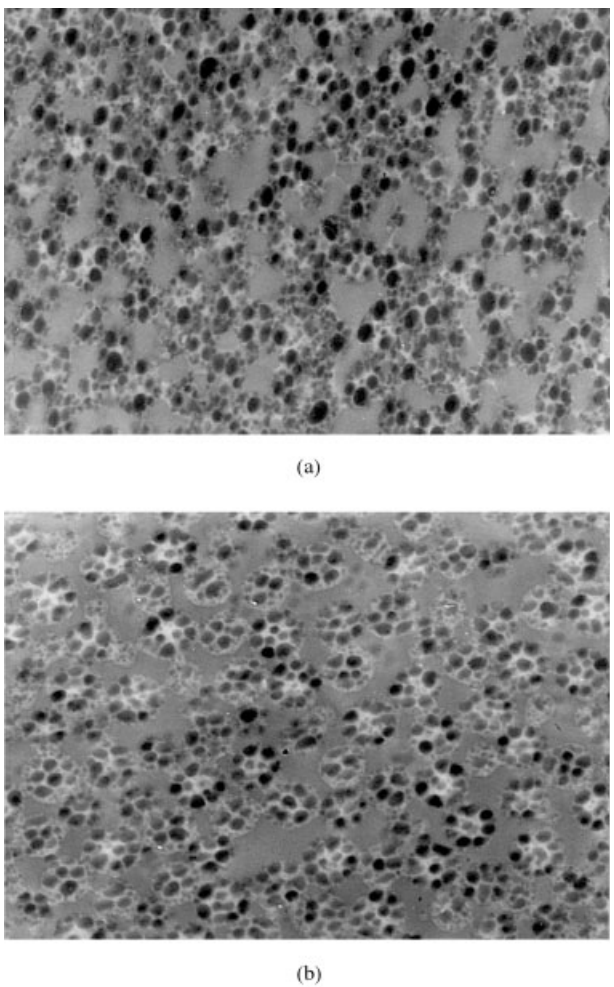

Figure 5 TEM photos of sectioned and stained samples of composite particles for the 70/30 PMMA/PMA seed polymer at T_g = 88°C. (a) Batch reaction with preswelled monomer; (b) batch reaction with unswelled monomer. Magnification 40,000×.

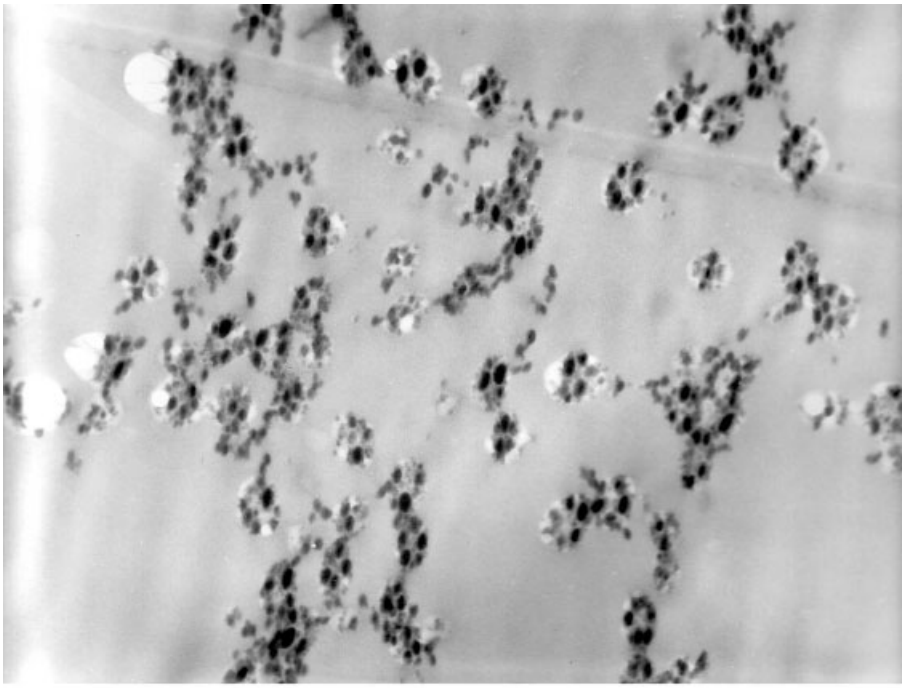

(a)

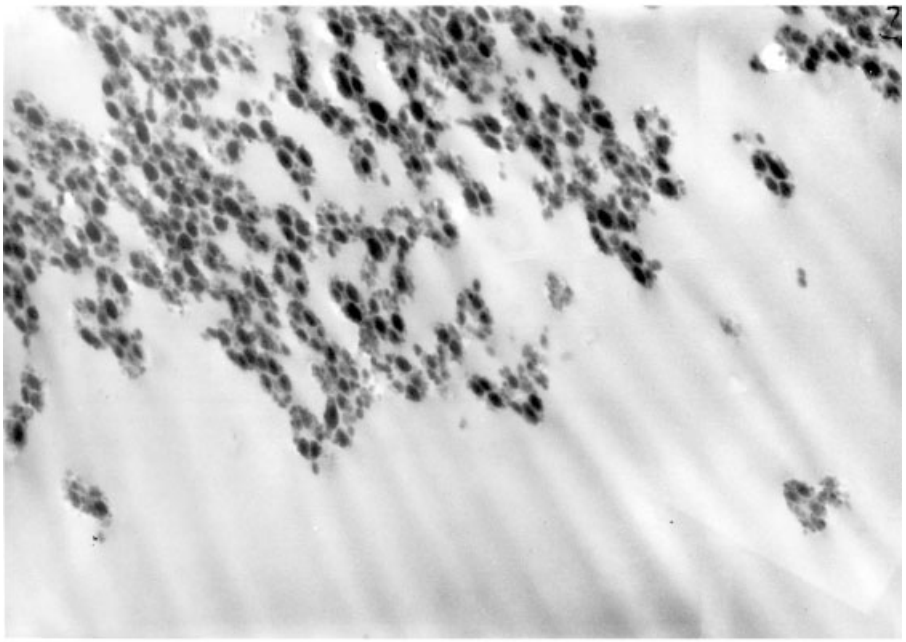

(b)

Figure 6 TEM photos of sectioned and stained samples of composite particles for the 60/40 PMMA/PMA seed polymer at T_g = 77°C. (a) Batch reaction with preswelled monomer; (b) batch reaction with unswelled monomer. Magnification 30,000×.

case, it is not surprising to see that as the monomer feed time is lengthened to 1.25 h and then to 4.2 h (all at a reaction temperature of 70°C), the morphology is a distinctive core-shell structure. This is shown clearly in Figures 7(a) and 7(b), where the particle cores are remarkably free of any PSt domains, indicating very little penetration of the entering oligomeric radicals. It should also be noticed that the shell is apparently composed of many separate PSt microdomains, having approximate sizes in the 30 nm range. We think that because of the very slow feed rate and the resulting low instantaneous monomer concentration in the particle, the microdomains did not have time to coalesce, and remain in a glassy, phase-separated state. Essentially the same can be said for the results for the 88°C T_g seed polymer reaction results as displayed in

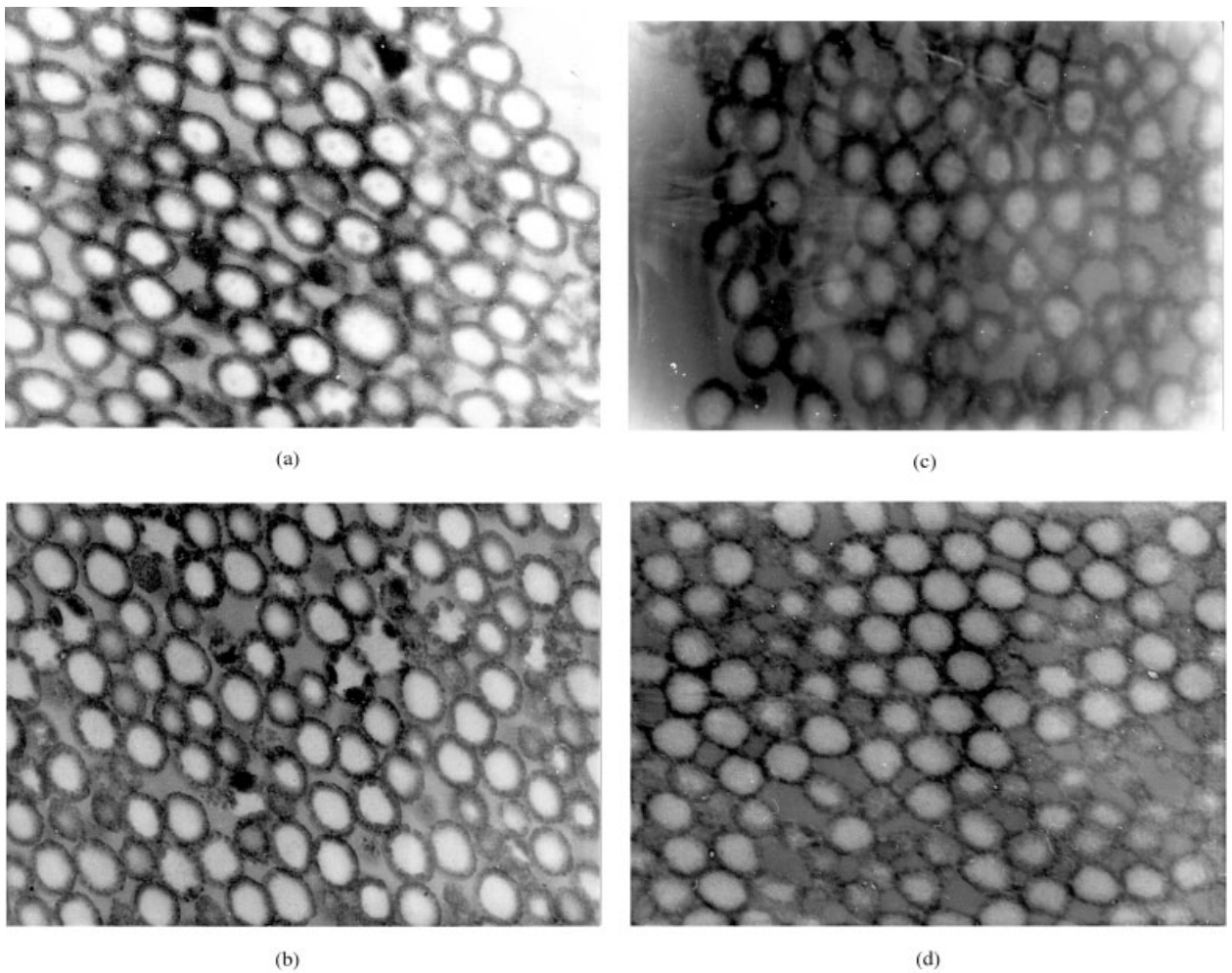

Figure 7 TEM photos of sectioned and stained samples of composite particles for semibatch reactions. (a) Seed polymer T_g = 98°C with monomer feed time of 1.25 h; (b) seed polymer T_g = 98°C with monomer feed time of 14.2 h; (c) seed polymer T_g = 88°C with monomer feed time of 1.25 h; (d) seed polymer T_g = 88°C with monomer feed time of 4.2 h; (e) seed polymer T_g = 77°C with monomer feed time of 4.2 h; (f) seed polymer T_g = 77°C with monomer feed time of 9.6 h; (g) seed polymer T_g = 52°C with monomer feed time of 4.2 h. All magnifications 40,000×.

Figure 5 and Figures 7(c) and 7(d). As we lowered the seed polymer T_g to 77°C, the second -stage reaction temperature was only 7°C below that T_g and the entering oligomeric radicals easily penetrated the particle core when the St monomer was flooded into the reactor, as shown by the results in Figure 6(b). As we extended the feed times to 4.2 and 9.6 h, we again obtained core–shell structures. Once again the shells were characterized by a noncontiguous phase structure. This is seen in Figures 7(e) and 7(f). The lowest T_g acrylic copolymer we tested was at 52°C and when used in the second-stage reaction at 70°C, the results showed that the entering oligomeric radicals were able to penetrate the seed particle to a substantial degree, as shown by the TEM micrograph in Figure 7(g). Here there is a fairly dense ring of PSt microdomains [larger in size than those in Figures 7(b–d) and (f)] at the periphery of the particle and some microdomains within the core of the particle.

As noted earlier, the initiator concentration in each second-stage reaction was adjusted to ensure that the radical entry rate to each particle was the same for each experiment. This and the fact that the particle sizes of the seed latices were close to the same allow us to be reasonably confident that for monomer feed times in the range of 4–9 h, the reactions were close to being "starve fed" at the 70°C reaction temperature. In then comparing the morphology results at the same monomer feed time, say 4.2 h, we ought to be able to clearly see the single effect of the seed polymer T_g on the ability of the oligomeric radical to penetrate the latex particle. This is seen quite clearly by comparing the TEM photos in Figures 7(b), 7(d), 7(e), and 7(g) for the seed polymers having T_gs of 98, 88, 77, and 52°C, respectively. Here we note the lack of significant penetration at a T_g only 7°C above T_r, but significant penetration at a T_g at 18°C below the reaction temperature.

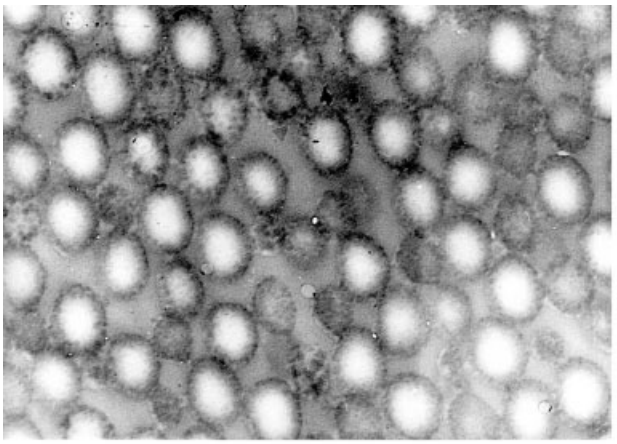

(e)

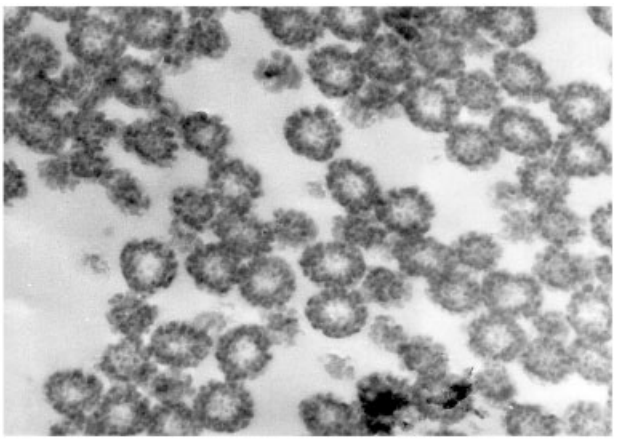

(g)

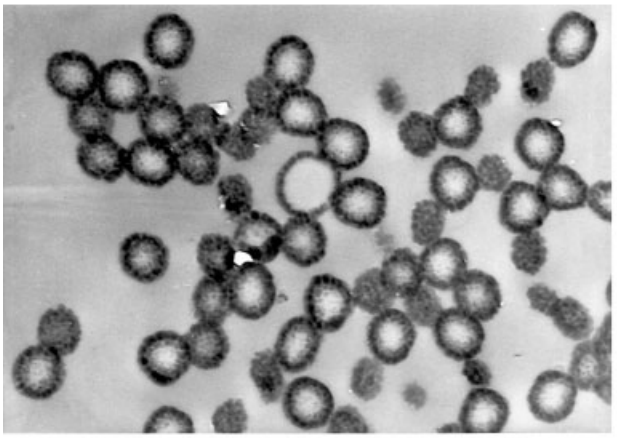

(f)

Figure 7 (*Continued from the previous page*)

One can also use variations in reaction temperature along with variations in seed polymer T_g to investigate the relationship of $(T_r - T_g)$ with morphology. Of course one needs to be cognizant of possible variations in instantaneous monomer concentrations among such reactions so as not to confuse the interpretations of the results. As noted above, this is realistic if the systems proceed to react under monomer starved conditions. Figure 8 shows the TEM photos for the T_g= 88°C seed polymer used for reactions at 70 and 60°C in (a) and (b), respectively. Here $(T_r - T_g)$ is −18 and −28°C, respectively, with both showing very well structured core-shell particles. In Figures 8(c) and 8(d) we present TEM photos for the T_g = 52°C seed polymer used for reactions at 70 and 50°C, respectively. Here at $(T_r - T_g)$ = + 18°C we see the effects of significant oligomeric radical penetration [as discussed earlier for Figure 7(g)], but very good core–shell features at $(T_r - T_g)$ = −2°C. This gives reasonable confirmation that one needs to have the seed polymer T_g somewhere about 15°C below the reaction temperature to allow the second-stage polymer to significantly accumulate within the core of the particle during the reaction.

Jönsson and Törnell[5,15] approached a similar goal in a different way, using a pure PMMA seed at very large particle sizes (ca. 500 nm) with St as the second-stage monomer. They used a calorimetric reactor capable of monomer feeding, and using both the directly measured reaction rate data and a material balance they could determine the instantaneous monomer concentration throughout the reaction. The T_g of the seed polymer "effective" during the reaction was determined by computing the T_g of the PMMA/St monomer "solution" within the seed particle at any time during the reaction. They used the method offered by Friis and Hamielec[16] to calculate limiting conversions in bulk, free radical polymerizations. With the aid of TEM photos they were able to determine the relationship between the effective T_g and the conditions at which they could see evidence of significant PSt penetration into the large seed particle. They concluded that this occurred when $(T_r - T_g)$ = +30°C, in slight

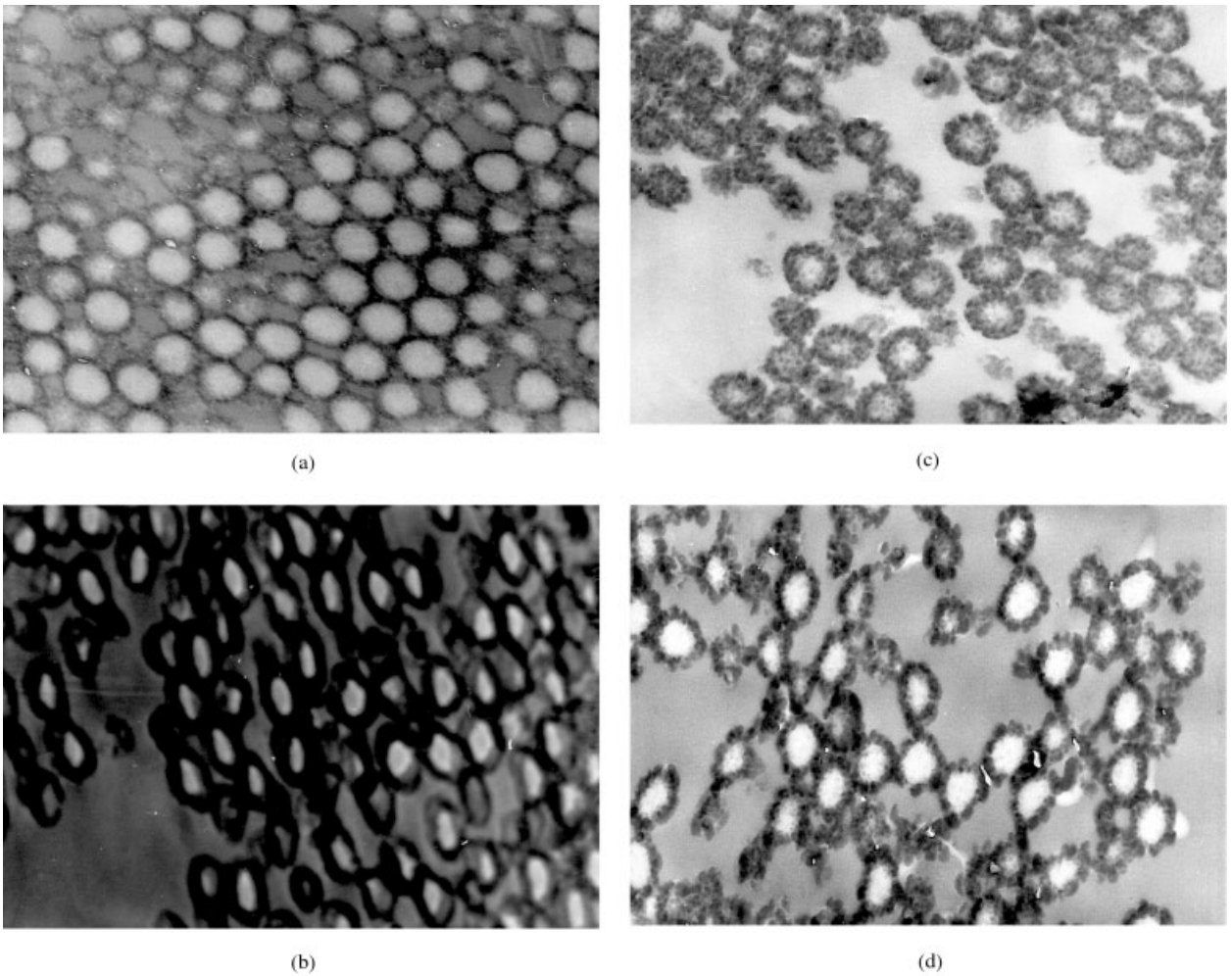

Figure 8 TEM photos of sectioned and stained samples of composite particles for semibatch reactions at monomer feed times of 4.2 h. (a) Seed polymer T_g = 88°C and T_r = 70°C; (b) seed polymer T_g = 88°C and T_r = 7060°C; (c) seed polymer T_g = 52°C and T_r = 70°C; (d) seed polymer T_g = 52°C and T_r = 50°C. All magnifications 40,000×.

contrast to the value of +15°C that we determined above.

Judging the effective glass transition temperature within the seed latex particle at any time during the reaction in order to assess the apparent diffusivity of the growing polymer radical is a good approach to predict the degree of penetration of the second-stage polymer. Unfortunately most reaction conditions do not yield instantaneous monomer concentrations, which remain constant throughout the monomer feed time. This is particularly true near the beginning of the process where the monomer builds up within the particle before any significant reaction takes place. Even the "starve-fed" conditions we noted above, while yielding low monomer concentrations, will produce local monomer concentrations that may vary

TABLE III
Calculated Results of T_r = 70°C

Seed polymer T_g (°C)	Monomer feed time (h)	Monomer concentration[a] (mol/L)	D_M (cm^2/s)	FP
98	4.2	0.60	$1.7 \cdot 10^{-12}$	0.13
77	9.6	0.16	$5.1 \cdot 10^{-12}$	0.11
52	4.2	0.45	$8.5 \cdot 10^{-9}$	0.41

[a] Increases rapidly from zero to a maximum value during the first 5–10% conversion and then decreases slightly during the monomer feed period. Values listed above are the average between the maximum and that at the end of the monomer feed.

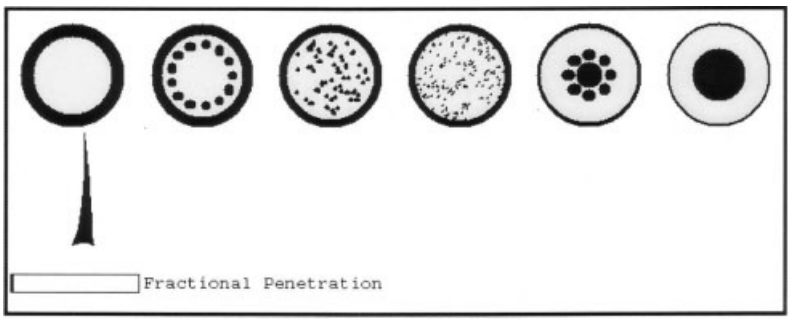

Figure 9 Schematically drawn particle morphologies (as in Fig. 2). Prediction represented by location of cursor for the experimental conditions associated with the seed polymer with T_g = 98°C as detailed in Table III.

substantially with reaction conditions. For that reason we have utilized Stubbs[4] methodology to calculate the fractional penetration (fraction of the radial distance the second-stage polymer radical diffuses over its lifetime, starting at the outside of the particle) for several of the experiments reported in this article. These calculations were applied to the entire reaction process and take into account the slight variations in seed latex particle size and the precise monomer feed rates among the various reactions. Table III shows the results of these calculations for the experiments utilizing three different seed polymers in the semibatch reaction mode at 70°C, with different monomer feed rates. The simulated experiments correspond to the morphology results shown in Figures 7(b) (T_g = 98°C, 4.2 h feed time), 7(f) (T_g = 77°C, 9.6 h feed time), and 7(g) (T_g = 52°C, 4.2 h feed time). As seen in the table, the average monomer concentrations in the particles were all fairly low (all below 8 wt % monomer), but differ substantially among the experiments. These values in combination with the T_g of the seed polymer yield monomer diffusivities that allow us to calculate the movement of the growing polymer chains according to eq. (3). Then using the relationship derived by Stubbs[4] for the fractional penetration, we are able to compare predictions to the experiments. As noted in Table III, the PSt is only forecast to penetrate about 12% of the radial distance for both the 98 and the 77°C T_g seed polymer cases, resulting in reasonably well-defined core–shell particles. This is in very good agreement with the TEM photos in Figures 7(b) and 7(f). The predicted pictograms (as in Fig. 2) for these simulations are given in Figures 9 and 10, respectively. Here the black cursors point to the place along the continuous scale (zero penetration at the far left and complete penetration at the far right) at which the second-stage polymer penetration is predicted. The particle structures drawn at the top are symbolic of certain degrees of penetration, but are not specific predictions of phase-separated polymers.[4] The fractional penetration for the 52°C T_g seed polymer case in Table III is slightly over 40% of the radial distance, predicting substantial amounts of PSt in the core of the particle. This result is shown in the pictogram in Figure 11 and agrees quite well with the TEM photo in Figure 7(g).

Together the results shown in Figures 4–8 and the qualitative and quantitative analyses presented above offer strong evidence that the seed polymer T_g, especially as it relates to the reaction temperature, has a strong influence on the resultant particle morphology. Our future computational efforts to predict nonequilibrium particle morphology center about the detailed consideration of three-dimensional diffusion (in spherical coordinates) of the entering oligomeric radicals. Clearly it is the combination of the seed polymer T_g, local monomer concentration, reaction temperature, and radical chain length that determine the dif-

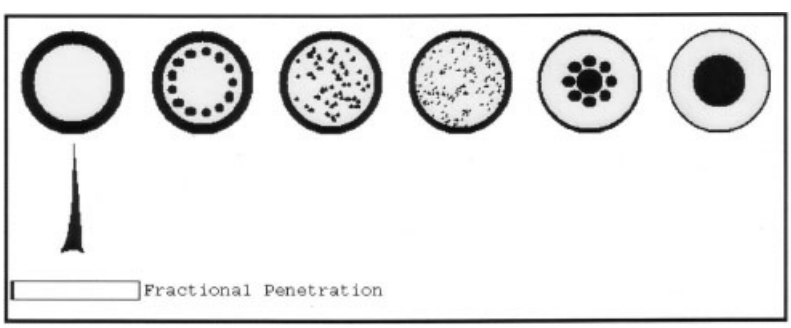

Figure 10 Schematically drawn particle morphologies (as in Fig. 2). Prediction represented by location of cursor for the experimental conditions associated with the seed polymer with T_g = 77°C as detailed in Table III.

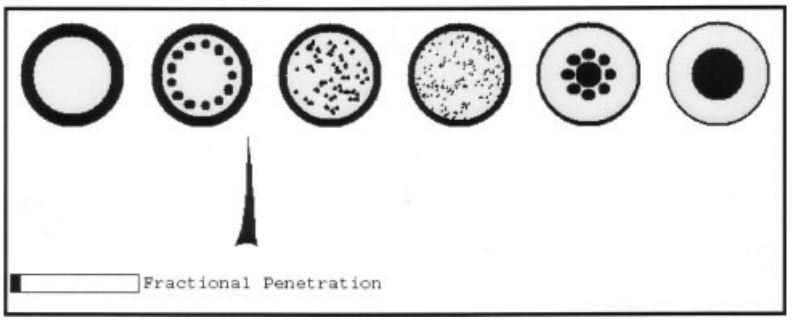

Figure 11 Schematically drawn particle morphologies (as in Fig. 2). Prediction represented by location of cursor for the experimental conditions associated with the seed polymer with T_g = 52°C as detailed in Table III.

fusion process. Since this process involves chemical reactions via propagation, possible chain transfer, and termination, there will also be an influence of the second-stage monomer type (via Kp, Kt, and perhaps Ktr) and radical entry rate (via initiator type and level, and T_r). Thus there is no absolutely correct answer to the question of which combination of seed polymer T_g and reaction temperature prevents significant penetration of the second stage polymer during the reaction. However, if we take a fractional penetration (FP) of 0.15 as a useful marker, the results of the experiments detailed above (for a particle size of about 300 nm) do offer a reasonable guideline that this FP will be exceeded when $(T_r - T_g) > 15$°C. Since an FP of 0.15 represents an absolute penetration depth (in nm) for large particles greater than that for small particles, the critical $(T_r - T_g)$ value is particle size dependent. In all cases $(T_r - T_g)$ must be smaller for small particles (leading to higher T_gs at a fixed T_r) than for large particles.

CONCLUSIONS

It is very clear that nonequilibrium particle morphologies are greatly varied due to the many different conditions that can effect the diffusion of the second-stage polymer within the host particle. Of the variables that control this diffusion, the T_g of the seed polymer is clearly one of the important ones. All of the experiments we conducted in this study resulted in nonequilibrium morphologies, and by controlling the monomer feed rates and radical entry rates into the seed particles we were able to create situations that could reliably demonstrate the independent effect of the seed polymer T_g. We conclude that at very low second-stage monomer concentrations (~ 5% or less) within the seed particle, one will generally achieve core–shell morphologies when the reaction temperature is at or lower than the T_g of the seed polymer. When that $T_g$is l5°C or more below the reaction temperature, there will be significant penetration of the second-stage polymer within the particle core, even at very low monomer concentrations. These results are reasonably predicted with the simple fractional penetration calculations presented earlier.[4]

We are thankful for the computational assistance of Jeffrey Stubbs of the University of New Hampshire, and for the TEM micrographs from Helen Hassander of Lund University.

References

1. González-Ortiz, L. J.; Asua, J. M. Macromolecules 1995, 28, 3135–3145.
2. González-Ortiz, L. J.; Asua, J. M. Macromolecules 1996, 29, 383–389.
3. González-Ortiz, L. J.; Asua, J. M. Macromolecules 1996, 29, 4520–4527.
4. Stubbs, J.; Karlsson, O.; Jönsson, J.-E.; Sundberg, E.; Durant, Y.; Sundberg, D. Colloids Surf, A 1999, 153, 255–270.
5. Jönsson, J.-E.; Hassander, H.; Törnell, B. Macromolecules 1994, 27, 1932–1937.
6. Sundberg, D. C.; Casassa, A. P.; Pantazopoulos, J.; Muscato, M. R.; Kronberg, B.; Berg, J. J Appl Polym Sci 1990, 41, 1425–1442.
7. Chen, Y. C.; Dimonie, V.; E1-Aasser, M. S. J Appl Polym Sci 1992, 45, 487–499.
8. Gilbert, R. G. Emulsion Polymerization: A Mechanistic Approach; Academic Press: San Diego, CA, 1995; p 29.
9. Fox, T. G. Bull Am Phys Soc 1956, 1, 123.
10. Dong, Y.; Sundberg, D. C. J Colloid Interfac Sci 2003, 258, 97.
11. Wu, S. Polymer Interface and Adhesion; Marcel Dekker: New York, 1982; p 105.
12. Durant, Y. G.; Sundberg, D. C. J Appl Polym Sci 1995, 58, 1607–1618.
13. Karlsson, O. J.; Stubbs, J. M.; Karlsson, L. E.; Sundberg, D. C. Polymer 2001,42, 4915–4923.
14. de Gennes, P.-G. Scaling Concepts in Polymer Physics; Cornell University Press: Ithaca, NY, 1979; p 227.
15. Jönsson, J.-E. Ph.D. thesis, Lund Institute of Technology, Lund, Sweden, 1994.
16. Friis, N.; Hameliec, A. Short Course on Polymer Production Technology; McMaster University: Hamilton, Ontario, Canada, 1976.